Supplemental Figure 1

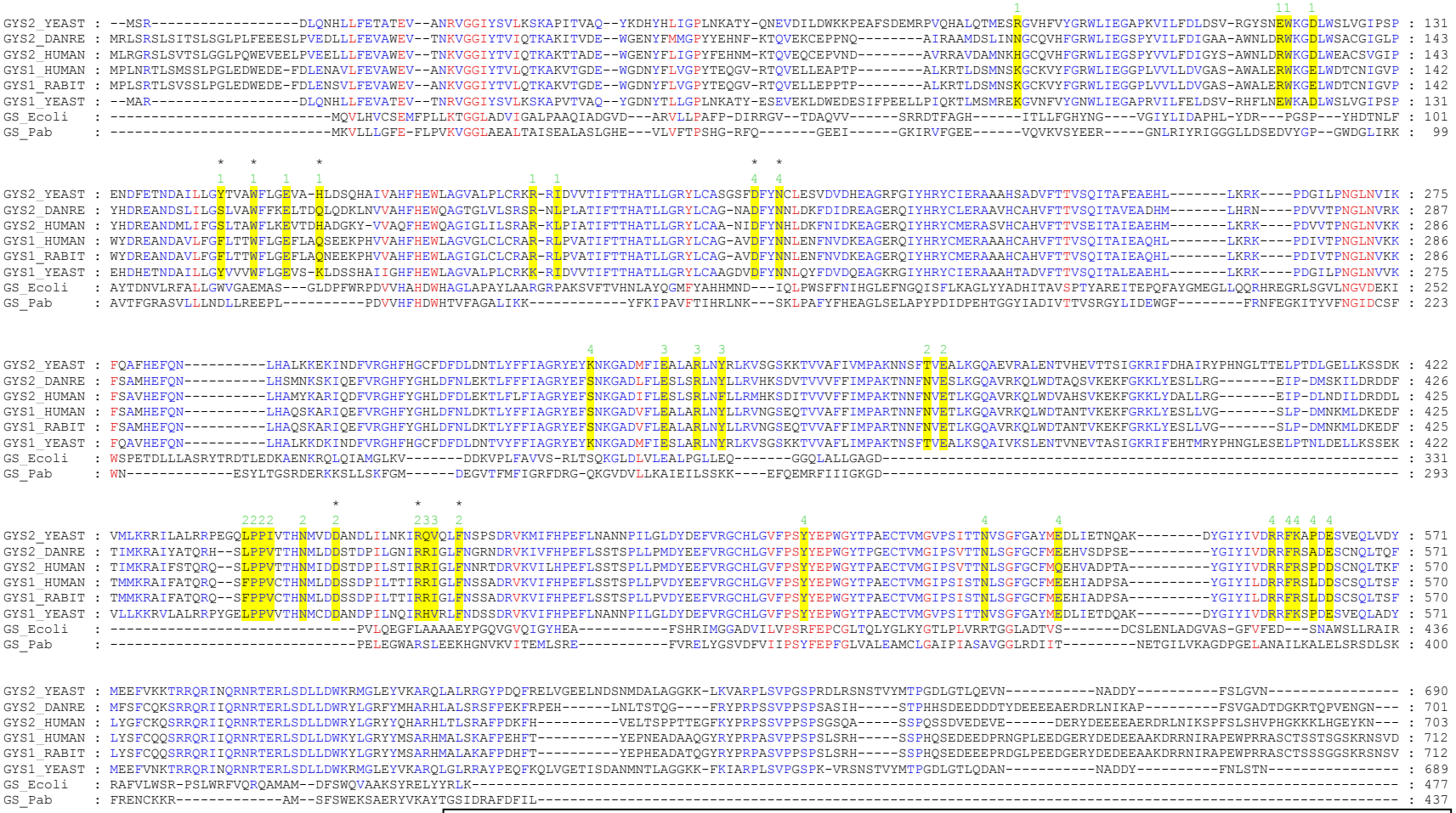

Supplemental Figure 1. Sequence alignment of glycogen synthase. A structure-based sequence alignment of the *E .coli* and *P. abyssi* glycogen synthase enzymes aligned to representative eukaryotic sequences. Red and blue font is used to denote residues that are conserved across species at 100% and 75%, respectively. Residues that contribute to maltodextran binding in yeast Gsy2p are highlighted in yellow. The binding site to which they contribute is indicated by the green numbers above each residue. Residues within each site that were mutated as part of this study are indicated with an asterisk above the site number. The multiple sequence alignment was generated using clustalW. A structure-based alignment of the *E. coli* and yeast enzymes was generated using LSQ superpose in Coot and used as the basis to manually edit the multiple sequence alignment produced by clustalW using the program GeneDoc.

Supplemental Figure 2

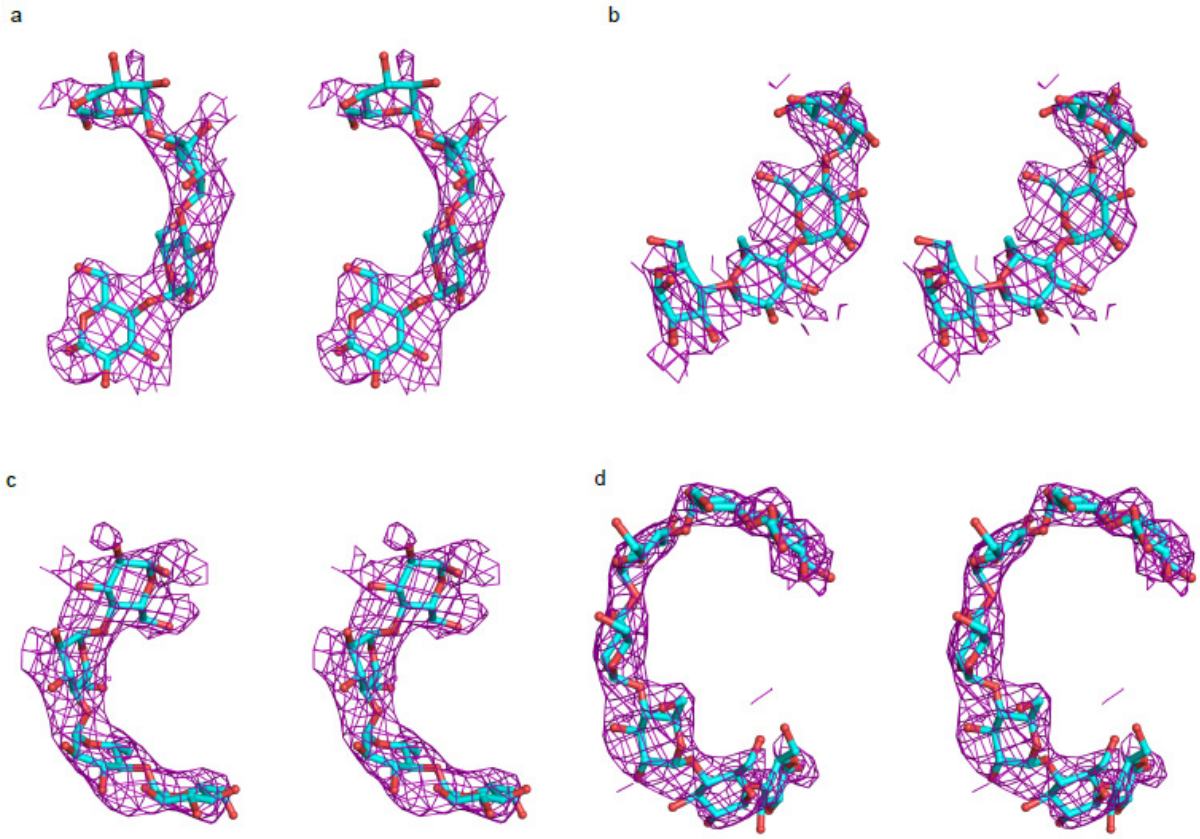

Supplemental Figure 2. Stereo diagram of the simulated annealing omit maps. Ball and stick representation of the bound oligosaccharides in site-1 (a), site-2 (b), site-3 (c) and site-4 (d). The electron density map shown is the simulated annealing omit map (contoured at 1standard deviation of the respective map).

Supplemental Figure 3

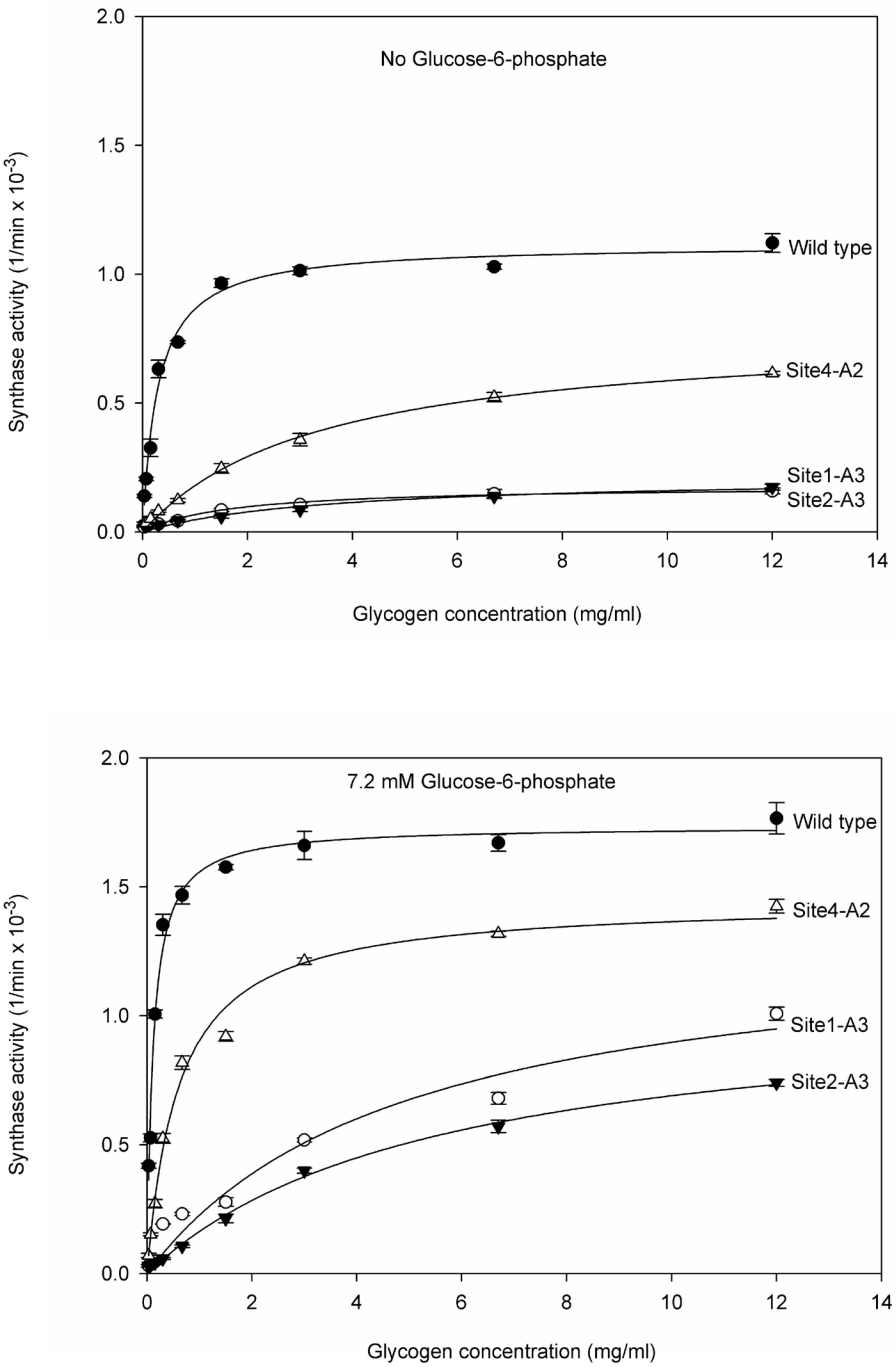

Supplemental Figure 3. Glycogen saturation curves for wild-type and mutant forms of Gsy2p. Michaelis – Menten plot of the enzyme assays for wild-type and mutant Gsy2p enzymes performed in the presence of 4.4 mM UDP-glucose using nine different concentrations of glycogen in the range of 0.03 – 12 mg/ml in the absence (a) and presence (b) of 7.2 mM glucose-6-phosphate. The data points for each curve represent the mean values from three independent experiments where each experiment contained duplicate measurements at each glycogen concentration. The error bars represent the standard deviations for the mean values.

Supplemental Figure 4

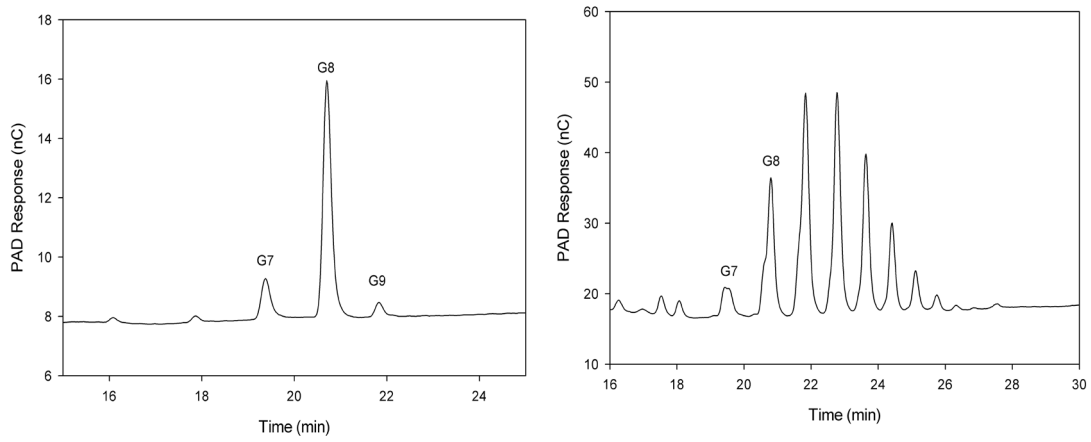

Supplemental Figure 4. HPAEC analysis of the product distributions produced following incubation of yeast Gsy2p with maltooctaose as a substrate. ***Panel A*** - A representative analytical trace for the HPAEC analysis of maltononaose production performed with wild-type Gys2p for 10 minutes at 30°C in 20 mM Tris, HCl, pH 7.6, 12.5 mM UDP-glucose, 50 mM maltooctaose and 1.3 μM enzyme. ***Panel B*** – A similar analytical trace performed using the wild-type Gsy2p enzyme for 4 hours at 30°C under the following conditions: 25 mM Tris-HCl pH 7.6, 12.5 mM UDP-glucose, 0.25 mM maltooctaose and 1.3 μM of wild type Gsy2p enzyme.

Figure 6

A

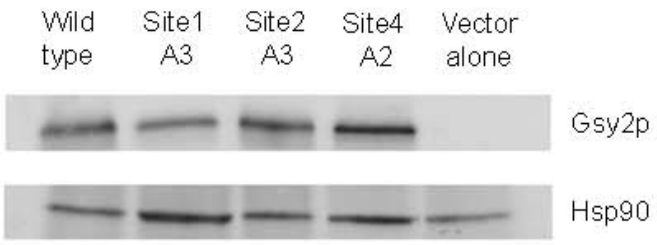

B

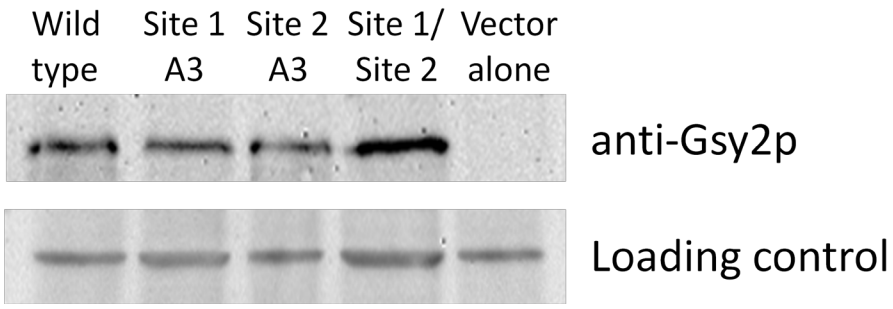

Supplemental Figure 5. Representative Western-blot demonstrating Gsy2p Expression in Δ*gsy1gsy2* yeast cells. ***Panel A***. Yeast cell extracts expressing the wild type and mutant enzymes were analyzed for Gsy2p expression using anti-GFP and Hsp90 was used as the loading control. Four independent experiments were performed and the expression levels were corrected based on the loading controls. After correction for loading differences, the levels of the WT enzyme in each blot was set to 1.0 and the relative expression levels for the mutants were determined for each blot and then averaged across all four blot experiments. The relative expression levels for the maltodextran binding site mutants was determined to be 0.7 ± 0.08 for the site-1 mutant (S1A3), 0.9 ± 0.09 for the site-2 mutant (S2A3), and 1.2 ± 0.16 for the site-4 mutant (S4A2). ***Panel B***. Yeast cell extracts expressing the wild type and mutant enzymes were analyzed for Gsy2p expression using anti-Gsy2p and Hsp90 was used as the loading control. The expression levels normalized to wild-type Gsy2p with this antibody are: 0.8 +/- 0.07 for site-1, 0.7 +/- 0.04 for site-2, and 1.3 +/- 0.21 for site-1/site-2.

Supplemental Table 1

Summary of Sugar polymer binding in Gsy2p structures

Subunit	No of ordered glucose molecules observed							
	Basal state conformation				Activated state conformation			
	Site-1	Site-2	Site-3	Site-4	Site-1	Site-2	Site-3	Site-4
A	4	4	-	-	-	-	2	7
B	4	4	-	-	-	-	-	-
C	-	-	-	-	3	-	-	-
D	-	-	-	-	-	4	4	-

Supplemental Table 2

Conformation of Oligosaccharide bound to Gsy2p

Subunit Site	Torsional angles		Glycosidic angle
	φ $O5_{(n+1)}$-$C1_{(n+1)}$-$O4_{(n)}$ -$C4_{(n)}$	ψ $C1_{(n+1)}$-$O4_{(n)}$-$C4_{(n)}$ –$C3_{(n)}$	τ $C1_{(n+1)}$-$O4_{(n)}$-$C4_{(n)}$
Basal Conformation			
A-site-1			
S1-S2	75.76	88.99	117.26
S2-S3	92.63	100.55	106.25
S3-S4	108.09	167.14	128.75
A-site-2			
S1-S2	94.53	103.71	110.22
S2-S3	93.85	115.85	106.71
S3-S4	97.91	104.31	115.24
B-site-1			
S1-S2	80.02	86.04	114.36
S2-S3	94.07	120.46	104.82
S3-S4	85.68	171.96	126.08
B-site-2			
S1-S2	84.85	97.99	107.93
S2-S3	92.17	134.21	113.48
S3-S4	91.15	170.30	118.91
Activated Conformation			
A-site-4			
S1-S2	102.87	93.20	116.39
S2-S3	117.70	108.55	114.28
S3-S4	93.73	93.42	116.17
S4-S5	95.00	105.24	112.52
S5-S6	98.23	103.46	117.37
S6-S7	112.34	101.58	117.36
A-site-3			
S1-S2	92.57	140.06	114.91
C-site-1			
S1-S2	78.26	86.01	112.70
S2-S3	103.97	111.33	113.24
D-site-2			
S1-S2	93.38	97.64	113.70
S2-S3	114.91	110.46	111.89
S3-S4	118.52	90.48	112.58
D-site-3			
S1-S2	103.70	98.02	111.70
S2-S3	107.76	125.46	114.52
S3-S4	123.17	94.73	113.51